

Predicting water level drawdown and assessment of land subsidence in Damghan aquifer by combining GMS and GEP models

Sakineh Parhizkar¹, Khalil Ajdary¹, Gholam Abbas Kazemi^{2*}, Samad Emamgholizadeh¹

¹ Faculty of Agriculture, University of Shahrood, Shahrood, Iran

² Faculty of Earth Sciences, University of Shahrood, Shahrood, Iran

*Corresponding author, e-mail: g_a_kazemi@shahroodut.ac.ir

(received: 17/02/2015 ; accepted: 01/06/2015)

Abstract

It is over two decades that groundwater flow models are routinely implemented for better management of groundwater resources. Modeling groundwater flow with the help of the ground water modeling system (GMS) in the Damghan plain aquifer in northern Iran, which experiences declining levels and numerous environmental hazards, has demonstrated that, (a) in the worst case scenario the aquifer will face 320 cm of drawdown by year 2019 and (b) land subsidence is observed mainly in areas that are subjected to an accelerated water level drawdown rate, such as, the southern part of the aquifer. Four different rainfall scenarios that have been modeled demonstrate that some areas of the aquifer are slightly impacted by climatic change in contrast to some other areas that are being influenced substantially. Together with GMS, Genetic Expression Programming (GEP) and Multiple Linear Regression (MLR) models were used to forecast land subsidence by applying developing functional relations to the long-term groundwater drawdown data. This segment of the study shows that a 35.4 cm and 39.45 cm settlement will occur if the groundwater level drops by 295 cm and 343 cm, respectively. This research shows that the water level in the Damghan aquifer continues to decline and the land subsidence will intensify. It is, therefore, needed to reduce groundwater pumping in high-risk areas.

Keywords: Ground Water Modeling, Damghan, Land Subsidence, Overexploitation, Water Level Drawdown.

Introduction

A model in any branch of science is a simplified device, which resembles the physical properties of the real specimen. Models provide an avenue to solve complex physical issues by using simple samples. In the study of subsurface water, any system that is capable of offering a valid estimate of the natural conditions governing groundwater flow is termed as a "model". A simulation of groundwater behavior that takes into consideration various parameters and properties of the aquifer is only possible through modeling (Bredehoeft & Hall, 1995; Gerla & Matheney, 1996; Varni & Usunoff, 1999; Nastevetal, 2005; Bedekar *et al.*, 2012). Although there are some questions about the ability of models in accurately representing the aquifer systems, and how complex models may be misleading (Voss, 2011), if a model is constructed properly, it can appropriately depict the relationship between hydrodynamic actions and reactions in an aquifer system. Hence, it helps to analyze the behavior and management of groundwater resources effectively.

Simulation of groundwater flow and transport by mathematical models has become widespread since the late 1970s. Models have been used for a variety of groundwater issues such as basin water management (Sakthivadivel, 2001), simulation of

the effect of subsurface barriers on the groundwater flow (Elago and Senth Kumar, 2006), groundwater management (Rejani *et al.*, 2008; Kushwaha *et al.*, 2008), and simulating a groundwater fall (Li *et al.*, 2011). A handful of examples of more recent researches in the field of groundwater modeling are described here. The application of GMS and MODFLOW in the Evan sub-basin of the semi-arid Khuzestan province in southwestern Iran was carried out by Sohrabi *et al.* (2013). They modeled various scenarios for a 10-year period, from 2005 to 2015, by assuming that the existing rate of groundwater draft and recharge will continue. The result of this modeling exercise indicated that the Evan sub-basin will face a decrease in the groundwater storage ranging from 4.43 to 8.34 MCM.

Louwyck *et al.* (2014) reported on an investigation that aimed to simulate an asymmetric groundwater flow in radially heterogeneous and layered aquifer systems, using the unmodified version of MODFLOW. They concluded that MODFLOW is capable of accurately simulating an asymmetric flow in such aquifer systems. Gurwin and Lubczynski (2005) used a ground water modeling system (GMS) to develop a conceptual model on the basis of data from several hundred boreholes and to calibrate a numerical-multi-

aquifer model. Results of their study showed that by setting up a conceptual model within the numerical model environment and by applying a quasi-3D solution, complex multi-aquifer systems can be well and efficiently modeled.

Yidana (2011) calibrated a groundwater flow model for some aquifers in the southern Voltaian sedimentary system (northern Ghana) under steady-state conditions. The result of the calibrated steady-state model suggested that aquifer hydraulic conductivities in the study area range from 1.19 to 6.3 m/day. Sun *et al.* (2011) investigated the numerical analysis of a 3-D regional groundwater flow model for the Nankou area in Beijing. The model calibration and sensitivity analysis were accomplished with inverse methods by applying a model independent parameter estimation system (PEST). The results of the calibrated model showed reasonable agreements with the observed water levels. The transient groundwater flow simulations reflect the observed drawdown of the past nine years and show the formation of a depression cone in an intensively pumped area.

Many cities and regions around the world have been heavily affected by groundwater associated land subsidence, for example, Venice (Lewis & Schrefler, 2007), Mexico (Ortega-Guerrero *et al.*, 1999), San Joaquin (Deverel & Leighton, 2010), Wairakei-Tauhara (O'Sullivan *et al.*, 2010), and China's Tianjin, Shanghai, and Jiangsu (Xue *et al.*, 2005). The rate of land subsidence has been reported to be up to 10 m in the California Central Valley (Williamson *et al.*, 1989, as cited in Huang *et al.*, 2012) and up to 3 m in the Houston (Texas) area (Kasmarek & Robinson, 2004, as cited in Huang *et al.*, 2012).

In Iran, a number of plains are being affected by land subsidence and are associated with severe damaging consequences (Rahmanian, 1986; Abbas Nejad, 1998; Fatemi Aghda *et al.*, 2001; Rahnama Rad & Firoozan, 2002; Lashkaripour *et al.*, 2006). For instance, in Rafsanjan in southeastern Iran, there are reports showing 42 cm of subsidence for each 10-m drop in the water table, and in nearby Sirjan, a 27-cm settlement for the same amount of water level drawdown has been recorded (Kerman Regional Water Company 2002). Mousavi *et al.* (2001) have shown that there is a direct correlation between land subsidence and the volume of extracted groundwater, and water level decline. In a study on land subsidence in southwest Tehran,

Tardast *et al.* (2011) have reported 21 cm of subsidence in the area, between 1995 and 2003, due to a water level drop.

In a slightly different, but closely related topic, Alkhamis *et al.* (2006) have found that land subsidence due to groundwater withdrawal is the cause of borehole failure in various plains in Iran. To further support such findings, Ghafouri *et al.* (2013) showed that in the Shabestar Plain in northwest Iran, water level drawdown and the associated land subsidence are the main causes of deterioration of water well screens.

With regard to implementation of models in the subsidence issue, Cui *et al.* (2014) developed a coupled numerical groundwater and land subsidence model for the Tianjin Plain in China. That model was employed not only to investigate the volume of groundwater resources and their changes over the last decade, but also to predict the changing patterns of the groundwater level and associated land subsidence. The simulation results demonstrated that if reduction in the groundwater withdrawal happens: (a) The groundwater level may gradually rise year by year, (b) the subsided land, in the subsidence affected regions, may rebound at an average rate of 2–3 mm/annum, and (c) the land subsidence rate in the other regions may start to decline. Despite these few examples, researches using mathematical models to predict land subsidence are few in number, given the severity of the financial losses associated with this phenomenon.

In Iran, which is an arid and semi-arid country, groundwater is the main source of water for agriculture, drinking, and industrial consumption. Consequently, the prediction of the groundwater level is necessary for better planning and management of the water resources (Emamgholizade *et al.*, 2014). In the study area, the Damghan aquifer in northern Iran, due to overexploitation and also the changing precipitation pattern and its quantity, the aquifer experiences rapid water level drawdown. The primary objective of this study is to examine the ability of GMS to predict rapid drops in the groundwater levels. Also, after calibration of the GMS model, four different rainfall scenarios have been used to predict the groundwater levels. More importantly, we aim to study groundwater driven land subsidence by the use of mathematical models. To achieve this goal, we combined GMS and other less used codes, such

as GEP and MLR, to predict the land subsidence rate in the Damghan aquifer (in the next five years), by developing functional relations to the long-term groundwater drawdown.

Study area

Damghan, with a population of 59,000, is a small city located 350 km to the east of the capital, Tehran, in northern Iran (Fig. 1). It is the largest population center in the Damghan district. The long-term average annual rainfall in Damghan is slightly over 120 mm, while average temperature is

15.8°C; therefore, it is categorized as an arid region on the basis of the De Martonne index and embrothermic curve. The water supply in the Damghan district is mainly through the groundwater resources, with the Cheshmeh Ali River, originating from the Cheshmah Ali spring, as the only permanent river in the area. The Cheshmah Ali River is dammed by the Shahcheraghi dam, located 12 km to the north of Damghan. The main use of water in the District of Damghan is in the agricultural sector, with pistachios as the primary product.



Figure 1. Location of the study area in northern Iran

Hydrogeology of Damghan Plain Aquifer

The Damghan plain, 1,173 km² in area, is a flat fertile land. On account of the large size of the Damghan plain aquifer, which is almost four times larger than the nearby Shahrood plain aquifer, the geological settings of the plain are quite complex and wide in range (Fig. 2). In the north, carbonate rocks are dominant, while in the northeast, marl and

gypsiferous formations are the main geological formations. The Damghan plain overlies the Damghan plain aquifer and is partly overlain by the Damghan city. It should be noted that the Qoushah plain is sometimes regarded as part of the Damghan plain. On account of this, in some references the area of the Damghan plain may be reported as slightly larger. The Damghan plain aquifer is

bordered by the Alborz mountain range to the north and the Damghan Kavir to the south ('Kavir' is a Persian term used to describe extensive flat saline lands). The general slope of the area is southward; surface waters originating from the northern mountains discharge into the southern Kavir. On account of lack of appreciable surface water resources, the pressure on groundwater resources in Damghan is immense. The hydraulic conductivity of the Damghan aquifer ranges from 3.43 to 11.6

m/day, and its specific yield varies substantially from 0.009 to 0.085 (Regional Water Authority of Semnan 2009). As per the Regional Water Authority of Semnan (2009), the average recharge rate to the Damghan plain is 10% of rainfall, taking into account (a) direct rainfall recharge, (b) reduction in groundwater withdrawal in rainy days due to decline in air temperature and evaporation rate, and (c) concentrated recharge in drainage lines and flood plain areas when there is surface runoff.

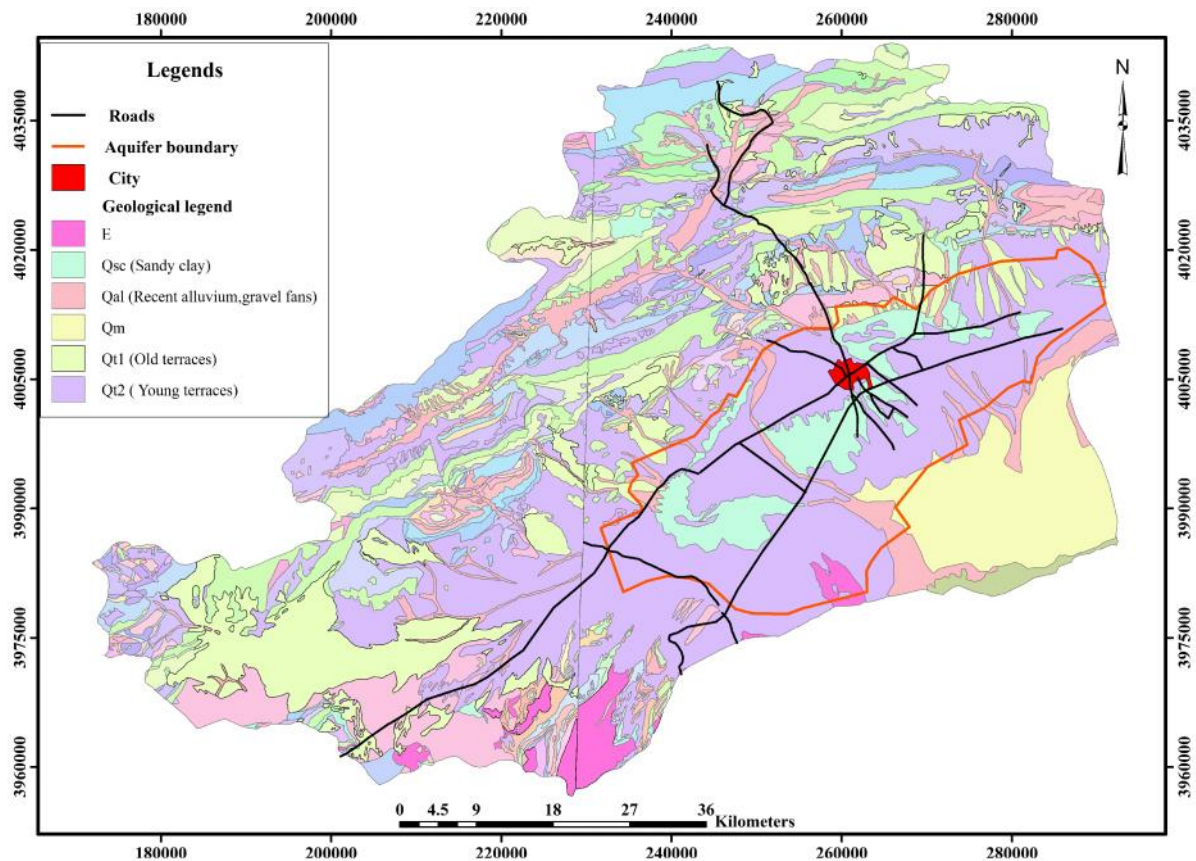


Figure 2. Simplified Geological map of the study area

Some 920 deep wells tap the Damghan plain aquifer and on an average extract 154 million cubic meters of water annually ($4.879 \text{ m}^3/\text{second}$). For this reason and also due to the long lasting drought, the water levels in the Damghan aquifer have been declining year after year. The water level map of the Damghan aquifer prepared on the basis of the 2012 water level records is shown in Figure 3. On the basis of this figure, northern, northeastern, and western boundaries are inflow boundaries, while the southern boundary acts as the outflow

boundary. These boundaries have been defined as the general head boundaries (GHB) in the developed model. The reason for defining such boundaries is because the water level in these boundaries is not constant, in contrast to the specified head boundary, and the water level could change due to internal stress. In addition, when calculated by hydraulic heads, the sensitivity of the model to the boundary conditions is less when the GHB are defined.

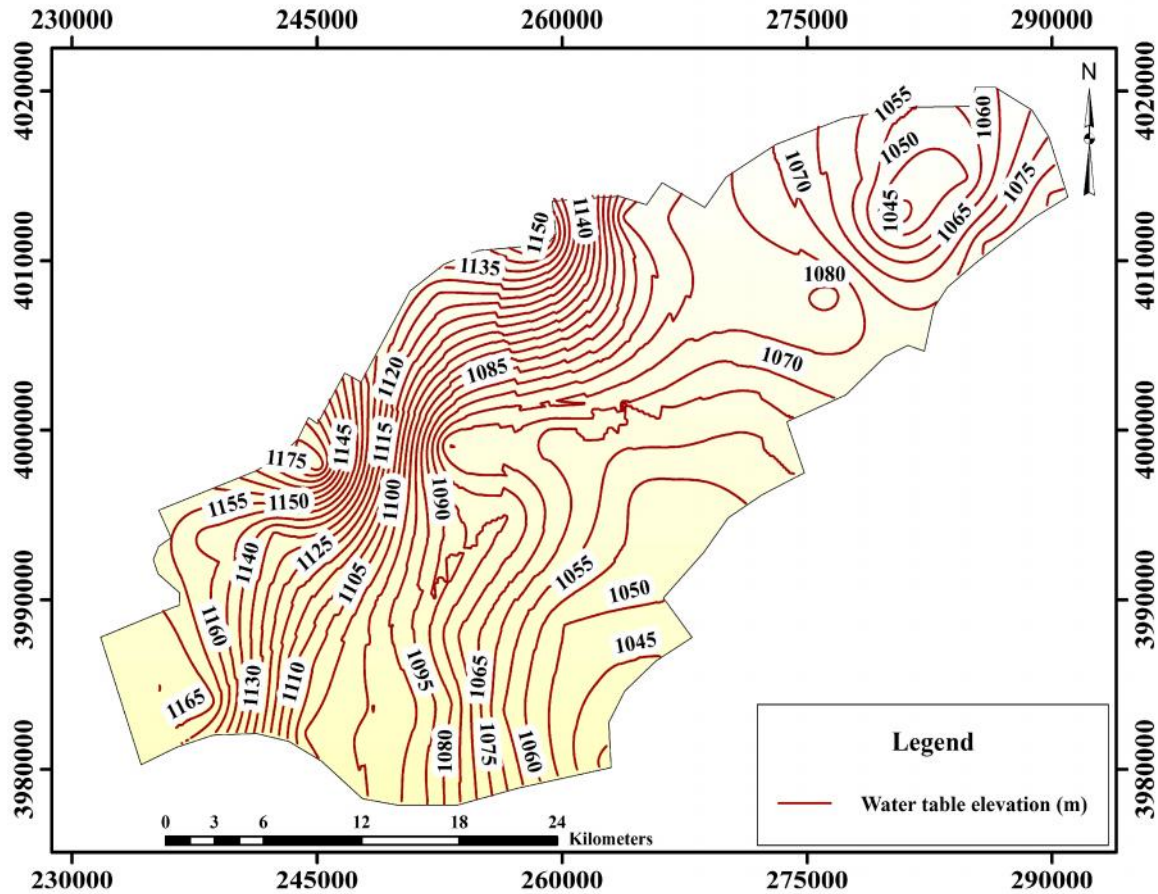


Figure 3. Water level map of the Damghan aquifer in 2012

Groundwater naturally occurs in the form of an unconfined and leaky aquifer. However, because of the extensiveness of the plain, the geometry and characteristics of these two aquifers are not well understood. Furthermore, excessive groundwater pumping during the past several decades and large drawdown rates has most likely caused these two aquifers to be hydraulically connected to the extent that at this point in time, it is safer to consider them as a single aquifer. One should also note that the two aquifers, through different components of the structures of drilled boreholes (pipes, casings, filter packs etc), can easily interact and swap a large volume of water. Also, the production wells and the piezometers have often been drilled fully intercepting the bedrock, and are often screened in their entire depth, preventing the authorities and the researchers from distinguishing the two aquifers. The depth to the bedrock ranges from 140 m in the southeastern part of the plain to 320 m in the northeastern part of the plain. In the southwestern part of the plain and also in the north of Damghan

city, the depth to the bedrock is approximately 260–280 m (Regional Water Authority of Semnan 2009).

Mathematical modeling

As a result of the complexity and numerous aquifer characteristics, problematic hydrogeological boundaries, and unknown geometry, the use of analytical models in simulating groundwater resources is generally limited. However, with the advance of computer codes and hardware, the applications of numerical models have expanded. In the first groundwater modeling study in 1968, in California, the finite difference model was employed to study the direction of groundwater flow in the coastal plain of Los Angeles (Spitz and Moreno, 1996). In finite difference models, a systematic grid is designed to divide the area under study into a number of polygons. Such models are widely in use in groundwater modeling exercises owing to the accessibility of computer codes, user friendliness, fitness to various aquifer conditions,

and relatively high accuracy. In the present study, because of the availability, the GMS 7.1 (MODFLOW code), which uses finite difference principles, has been employed to model the Damghan aquifer. The first step in any hydrogeological modeling exercise is the

development of a conceptual model that identifies hydrostratigraphic units and system boundaries, and usually includes a field visit. Figure 4 depicts the location of both production and monitoring bores and has been used as a base for the conceptual model of the study area.

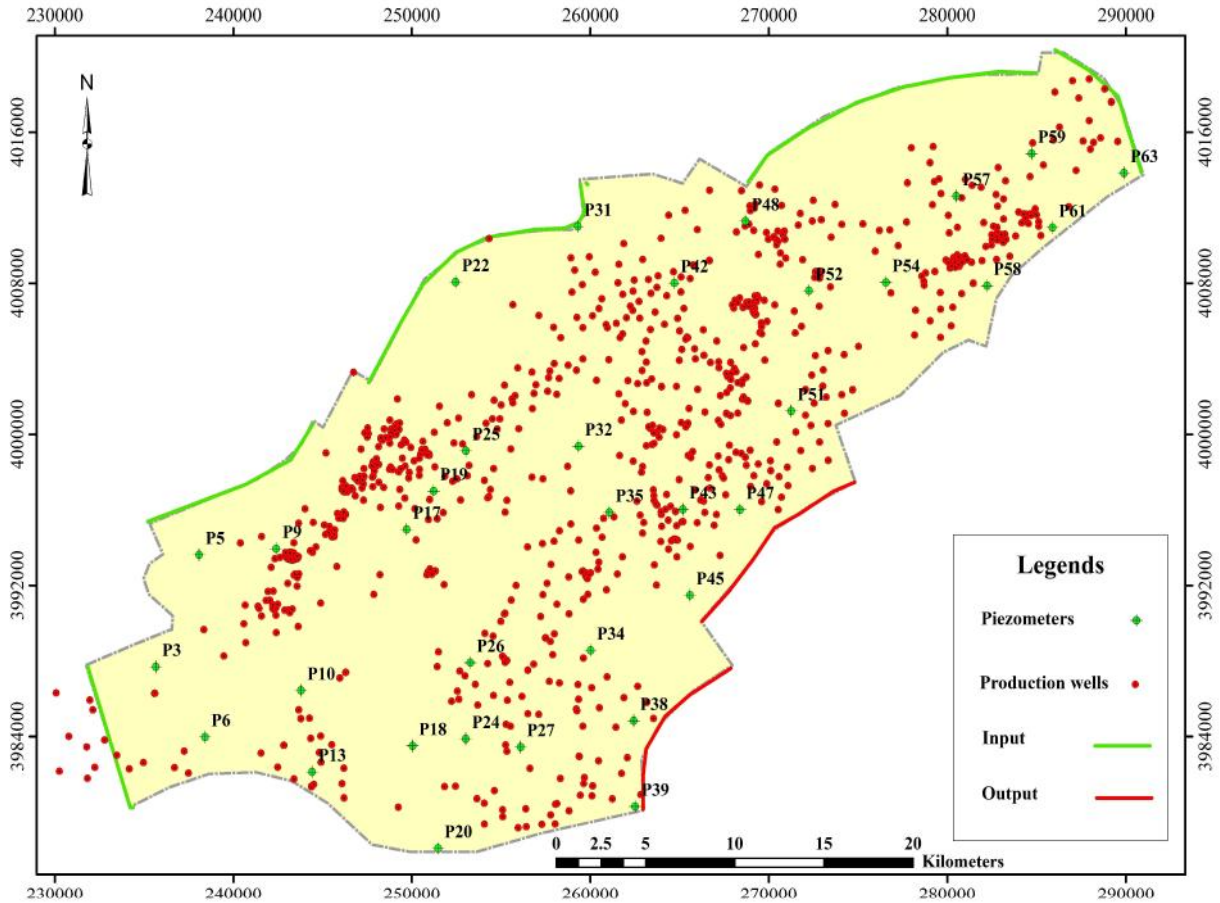


Figure 4. Location of production bores, piezometers, and inflow and outflow boundaries. This map is the basis of the conceptual model of the study area

Mathematical equations

In steady state conditions where inputs into an aquifer equal the outputs, there will be no change in the volume of aquifer storage. Consequently, the piezometric heads do not fluctuate with time and the Laplace equation will be as follows:

$$\frac{\partial^2 h}{\partial x^2} + \frac{\partial^2 h}{\partial y^2} + \frac{\partial^2 h}{\partial z^2} = 0 \quad (1)$$

The governing equation in unsteady state conditions in a heterogeneous confined aquifer is:

$$\frac{\partial}{\partial x} \left(K_{xx} \frac{\partial h}{\partial x} \right) + \frac{\partial}{\partial y} \left(K_{yy} \frac{\partial h}{\partial y} \right) + \frac{\partial}{\partial z} \left(K_{zz} \frac{\partial h}{\partial z} \right) = S_s \frac{\partial h}{\partial t} \quad (2)$$

For homogeneous confined aquifers, the above equation is summarized in the form of:

$$K_x \frac{\partial^2 h}{\partial x^2} + K_y \frac{\partial^2 h}{\partial y^2} + K_z \frac{\partial^2 h}{\partial z^2} = S_s \frac{\partial h}{\partial t} \quad (3)$$

If the aquifer is assumed to be homogeneous ($K_x = K_y = K_z = K$), Equation 3 transforms to:

$$\frac{\partial^2 h}{\partial x^2} + \frac{\partial^2 h}{\partial y^2} + \frac{\partial^2 h}{\partial z^2} = \frac{S_s}{K} \frac{\partial h}{\partial t} \quad (4)$$

For unconfined aquifers, by substituting S_y for S_s , the governing equation for groundwater flow will be:

$$\frac{\partial}{\partial x} \left(h \frac{\partial h}{\partial x} \right) + \frac{\partial}{\partial y} \left(h \frac{\partial h}{\partial y} \right) + \frac{\partial}{\partial z} \left(h \frac{\partial h}{\partial z} \right) = \frac{S_y}{K} \frac{\partial h}{\partial t} \quad (5)$$

The above equation is the Boussinesq's nonlinear partial differential equation, which is difficult to solve by analytical techniques owing to its nonlinear characteristics.

When different rates of recharges and discharges take place in an aquifer system, the general function of W is added to the right side of the Boussinesq's equation, in which the plus sign is the indication of discharge and the minus sign represents recharge. In three-dimensional conditions, function W is an indication of the discharge rate for length, area, and volume, respectively, which is:

$$\frac{\partial}{\partial x} \left(Kh \frac{\partial h}{\partial x} \right) + \frac{\partial}{\partial y} \left(Kh \frac{\partial h}{\partial y} \right) + \frac{\partial}{\partial z} \left(Kh \frac{\partial h}{\partial z} \right) = S_y \frac{\partial h}{\partial t} \pm W \quad (6)$$

Since a long time, water levels in the Damghan aquifer have been monitored via 40 piezometers. From year 2011 onward, six piezometers have dried up, and are no longer monitored. Consequently, in this modeling exercise, the historical records of only 34 piezometers have been used for both steady and transient conditions. By screening all available piezometric data in all these years, the best period for the initial values was chosen as September 2006, and the best period to run in steady state conditions was October 2006–March 2007, and for unsteady state conditions April 2007–March 2011. For the prediction of dry, wet, and normal periods, April 2014–March 2019 were selected. For simulating flow by the finite difference method, the study area has been divided into a number of cells. The dimensions of the cells should be selected properly in order to reduce computational times as well as to achieve more realistic results. The designed grid of the mathematical model of the Damghan aquifer, which is determined by the trial

and error method, contains $1000 \text{ m} \times 1000 \text{ m}$ cells; it is made up of 31 rows and 65 columns, which are of a block-centered type.

Calibration and validation of the ground water modeling system model

Before using any model for the prediction of the groundwater level, the model must be calibrated and validated with different piezometric data. In this study, the model was calibrated for the 2004–2009 year data and validation was based on the 2009–2014 data. The performance of the GMS model was evaluated based on four statistical parameters, namely *RMSE* (root mean square error), *NRMSE* (Normalized RMSE), *d* (agreement index), and *E* (Nash-Sutcliffe modeling efficiency), and these have been examined. These metrics can be shown by:

1. Root mean square error (RMSE)

$$RMSE = \left\{ \frac{1}{n} \left[\sum_{i=1}^n (X_i - Y_i)^2 \right] \right\}^{0.5} \quad (7)$$

2. Normalized RMSE (NRMSE)

$$NRMSE = \frac{\left[\frac{1}{n} \sum_{i=1}^n (X_i - Y_i)^2 \right]^{0.5}}{O} \quad (8)$$

where, n represents the number of observations, X represents the measured values, Y represents the estimated values, and O represents the mean values of the measured data.

3. Agreement index (d)

$$d = 1 - \left\{ \frac{\sum_{i=1}^n (X_i - Y_i)^2}{\sum_{i=1}^n (|X_i - O| + |Y_i - O_e|)^2} \right\} \quad (9)$$

where d is the index of agreement and O_e is the mean value of the estimated data.

4. Nash-Sutcliffe modeling efficiency (E)

$$E = 1 - \left\{ \frac{\sum_{i=1}^n (X_i - Y_i)^2}{\sum_{i=1}^n (X_i - O)^2} \right\} \quad (10)$$

The value of NRMSE and d approaches 0.0 and

1.0, respectively, for accurate estimation. The closer *NRMSE* is to 0, the more accurate the model is. The value of *d* varies between 0 and 1.0 and the closer its value to 1.0, the more accurate the model is. Modeling efficiency (*E*) ranges from $-$ to 1. An efficiency of 1 corresponds to a perfect match between the modeled and observed data. $E = 0$ indicates that the model prediction is as accurate as the mean of the observed data.

As mentioned, prior to running the model for main calculations to predict changes in the groundwater level under different conditions, the

GMS was calibrated with different piezometric data. Figure 5 shows the calibration results and Figure 6 shows the validation results. Different statistical parameters for four piezometers, located in various parts of the study area are shown in these figures, demonstrating that all the statistical parameters show perfect results. After obtaining these results, we used the model for the main objective, which is the prediction of water level in different parts of the plain under diverse climatic scenarios.

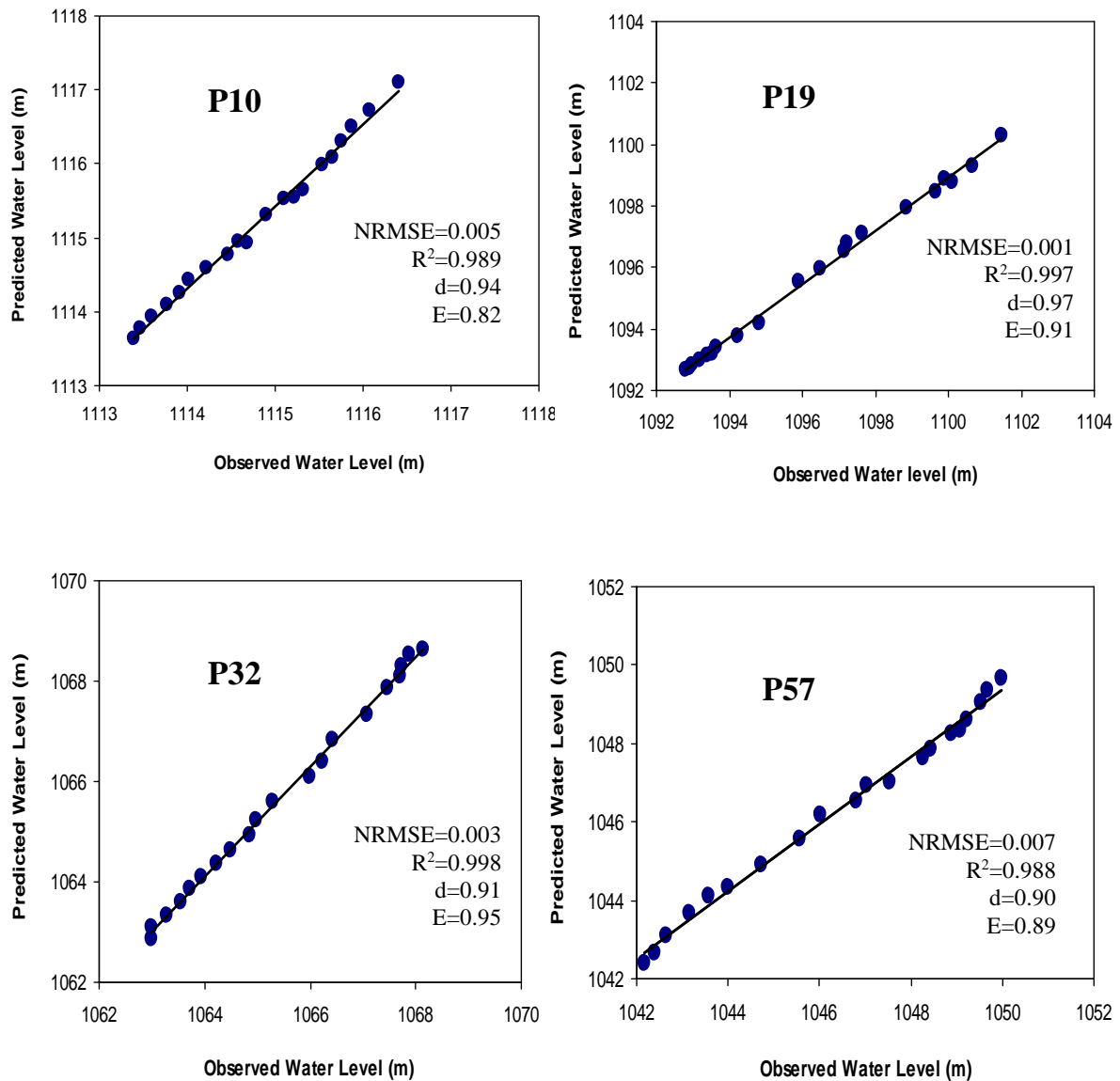


Figure 5. The correlation between the observed and predicted water levels in the calibration stage of GMS

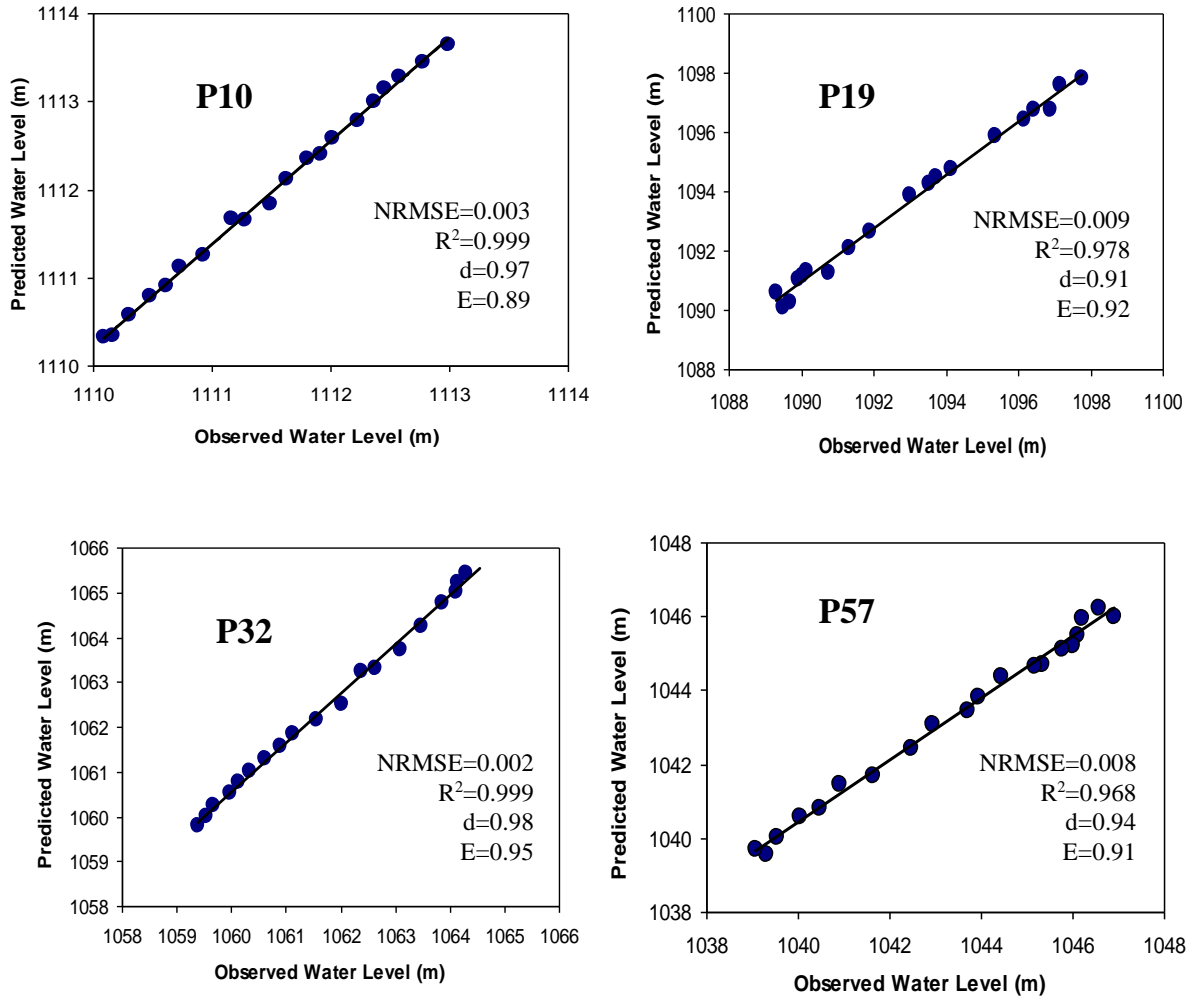


Figure 6. The correlation between the observed and predicted water levels in the validation stage of GMS

Results and Discussion

Prediction of groundwater drawdown

The modeling results have shown that the Damghan aquifer can be divided into three separate regions on the basis of the ranges of the recorded drawdown values; northern, southern and central regions. In this section, the predictions for various scenarios in the three mentioned regions are discussed. It is necessary to point out that the model was run to forecast four different scenarios within the next five years, 2014–2019, including:

- Continuation of the present conditions (normal)
- Occurrence of drier periods
- Increase in the rainfall to as much as 1.5 times that of the current annual average.
- Increase in the rainfall to as much as twice that of the current annual average.

Results for northern region

Figure 7 illustrates the expected changes in the water level in eight piezometers located in the northern region of the plain (Piezometer Nos. 31, 48, 57, 59, 22, 42, 58, 61). This figure shows that there is no difference between the various scenarios in the northern region, and in all scenarios there would be 3.16 m of drawdown. Such a situation, where there is no difference between various scenarios, is observed in this region only. The reason for this unusual behavior is that the piezometers in this region are located close to the plain margin, and the local groundwater extraction rate is higher. Therefore, it seems that the only mitigation measure applicable for this region is abandoning the production wells and stopping groundwater withdrawal.

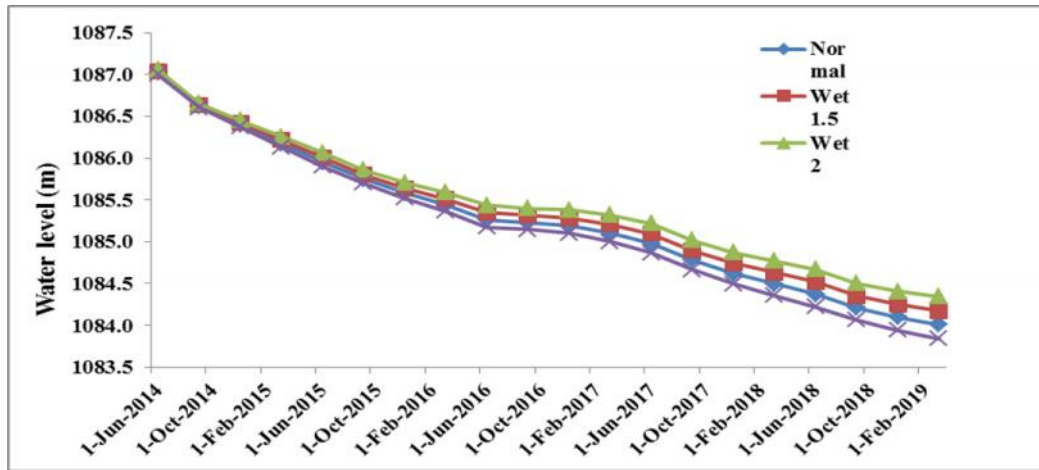


Figure 7. Average water level elevation in Piezometer Nos. 61, 58, 42, 22, 59, 57, 48, 31 for the four different modeled scenarios north of the Damghan plain

Results for southern region

In Figure 8, the average predicted drawdown for eight piezometers in the southern region of the plain is shown. This figure shows that if dry years prevail in the coming years, there would be a

drawdown of 2.82 m in the southern region of the plain. It also shows that in the case of normal rain, there would be 2.65 m of decline in the water level. If rainfall becomes double, the drawdown would then reduce to 2.31 m

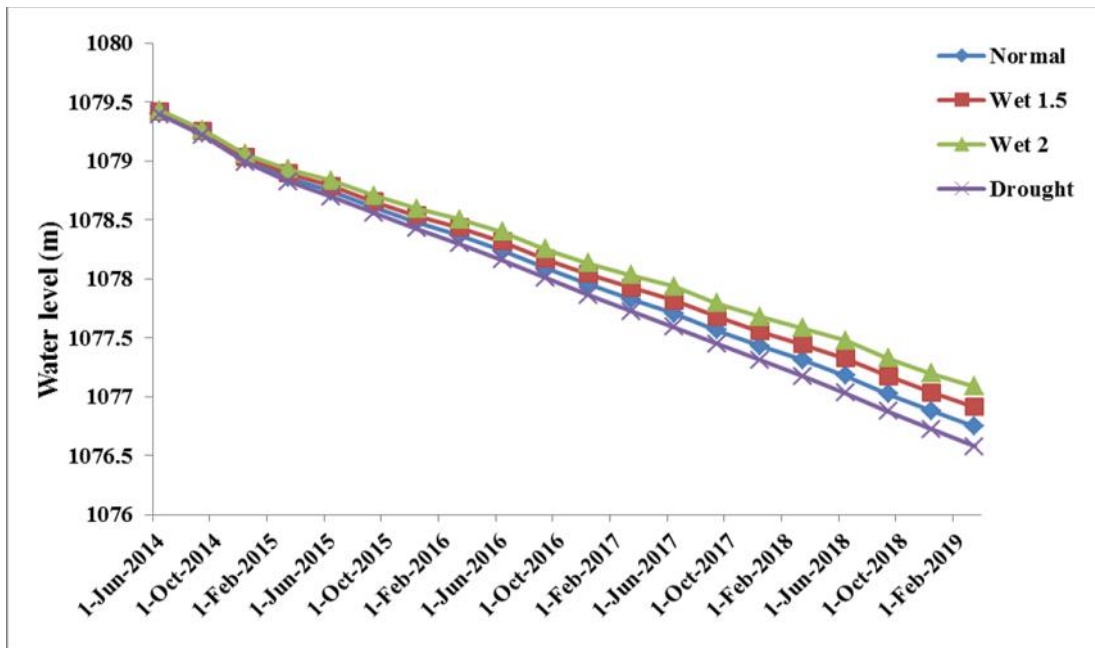


Figure 8. Average water level elevation in Piezometers Nos. 39, 38, 20, 13, 27, 24, 18, and 10 for the four different modeled scenarios south of the Damghan plain

Results for central region

The results of model prediction for the central zone of the plain in Figure 9 show that there would be 3.43 m of drawdown by the next five years in this region. Such conditions would definitely impact the

plain severely. If normal rainfall condition continues, there would be 2.95 m of decline, and in the case of a 1.5- to 2-fold increase in rainfall, the decline in water level would be 2.27 m.

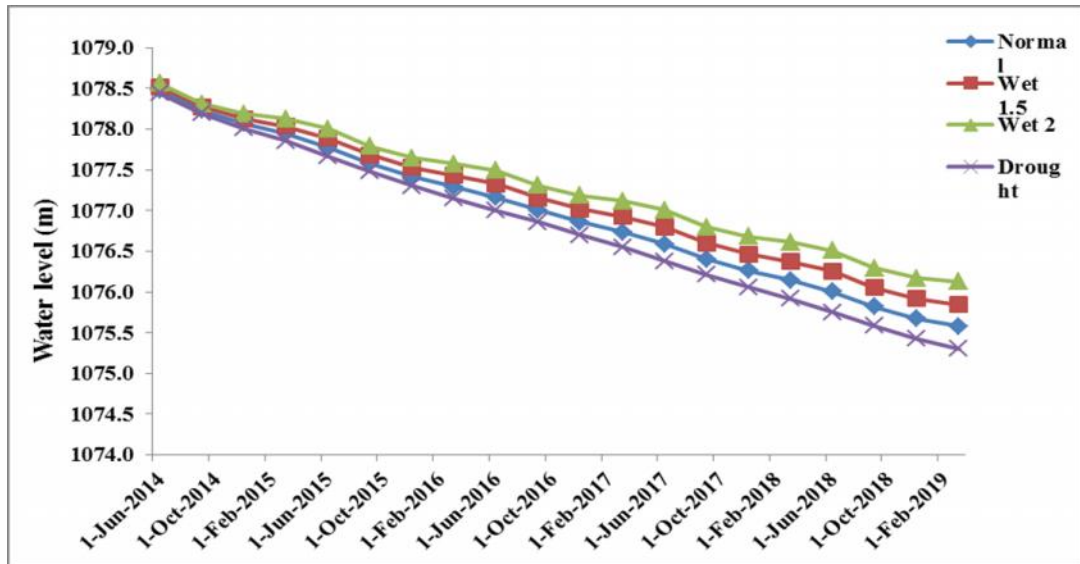


Figure 9. Average water level elevation in Piezometers Nos. 51, 47, 43, 17, 35, 32, 25, and 19 for the four different modeled scenarios in the central part of the Damghan plain

Results for the entire plain

Figure 10 shows groundwater conditions in the plain as a unified entity. On the basis of this figure, if drought prevails, the water level will drop by 3.43 m in five years. If the current situation continues, there will be 2.87 m of drawdown. Also, based on the same figure, with 1.5 times increase in the average annual rainfall, 2.6 m, and with twice the increase in rainfall amount, 2.32 m of

drawdown will be encountered. In such cases, the aquifer will be considerably damaged. By multiplying the area of the plain by the storage coefficient and drawdown value, approximately 176 MCM ($3 \text{ m} \times 0.05 \times 1173.55 \text{ km}^2 = 168.4 \text{ MCM}$) of the aquifer storage will be lost. This storage is not likely to be replaced easily considering the current prevailing drought in the region.

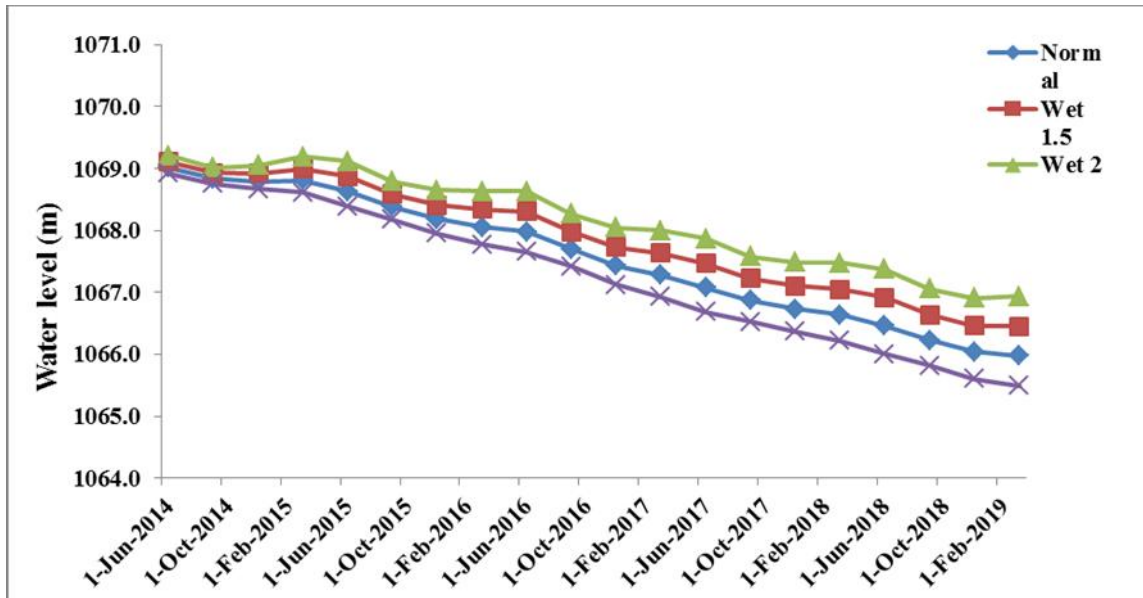


Figure 10. Average water level elevation in all 24 piezometers for the four different modeled scenarios in the Damghan plain

Prediction of land subsidence

There are reports (M. Shakeri, Personal communication, 2015) showing various amounts of land subsidence in the Plain of Semnan (10–12 cm/year), Plain of Garmsar (8 cm/year), and Plain of Eyvanakey (12 cm/year). Field investigation shows that evidences of land subsidence in the southern region of the Plain of Damghan are ample. Subsidence affected region is 180 km² in area and is bounded by 247000–265000 easting and 3980000–3990000 northing (Fig. 11). The subsided area comprises 15% of the plain area. The lithology of this area, as shown in the drilling logs,

is mainly clay, sand, and sandy clay (Fig. 12). Gradual land subsidence in this area has led to the appearance of long earth cracks, which are a few hundred meters in length and up to one meter in width. Such cracks have caused considerable financial loss to the rail roads and other infrastructures. Further subsidence-induced damages include:

- Apparent lengthening of water well screens
- Emergence of sink holes
- Damage to water well screens
- Reduction in the quality of groundwater

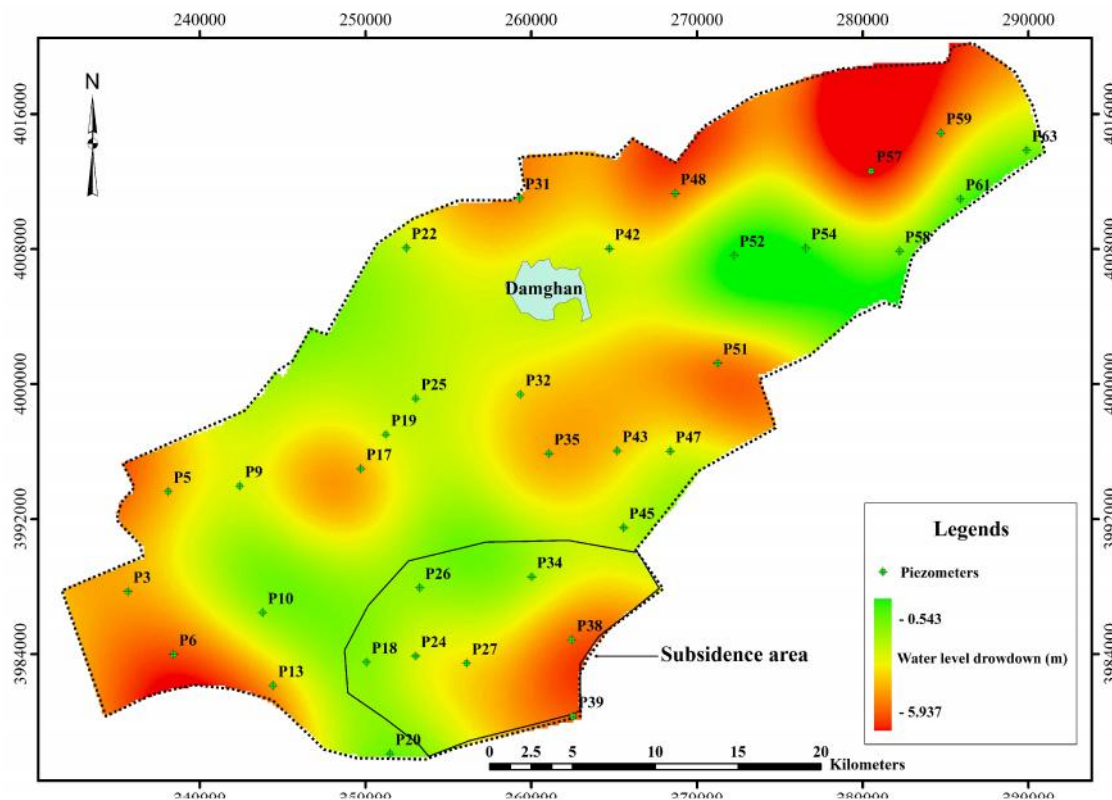


Figure 11. Spatial distribution of the water level drawdown and the location of the subsided area

Land subsidence in the southern part of the Damghan plain has occurred as a result of severe groundwater overdraft, excessive number of pumping wells, and a type of lithology, which is dominantly clay (Figs. 13 and 14). There are 69 deep production bores in this region extracting 400 l/s of water. On the basis of the local water authority report, there has been approximately 5 m of drawdown during the years 2001–2011 (Semnan Regional Water Company, 2012), which is extremely significant. On the basis of field

observation and aerial photographs, the amount of subsidence decreases westward. Farmers strive to fill the cracks with soil to prevent them from becoming enlarged. If the drought continues, and if the groundwater abstraction rate remains the same, it is very likely that the subsided area is enlarged. The drawdown values forecasted for the subsided area are shown in Figure 15. As seen in Figure 15, the amount of drawdown in the worst case scenario in the subsided region would be 2.85 m.



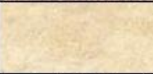

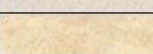
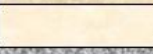





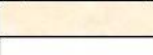
Sediment type	Legend	Depth (m)	Borehole Geometry
Sand (fine-grain)		10	
Sandy clay		20	
Sand with fine gravel		30	
Clay sand		40	
Sandy clay		40	
Clay		40	
Fine to medium grained sand with fine gravel		50	
Fine-grained gravel		60	
Clay sand		70	
Sand, fine gravel		80	
Clay		90	
		90	

Figure 12. Geological log of Masih Abad Piezometer (X = 262520, Y= 3980303) as an example



Figure 13. Photo of a long wide crack formed due to land subsidence south of the Damghan plain

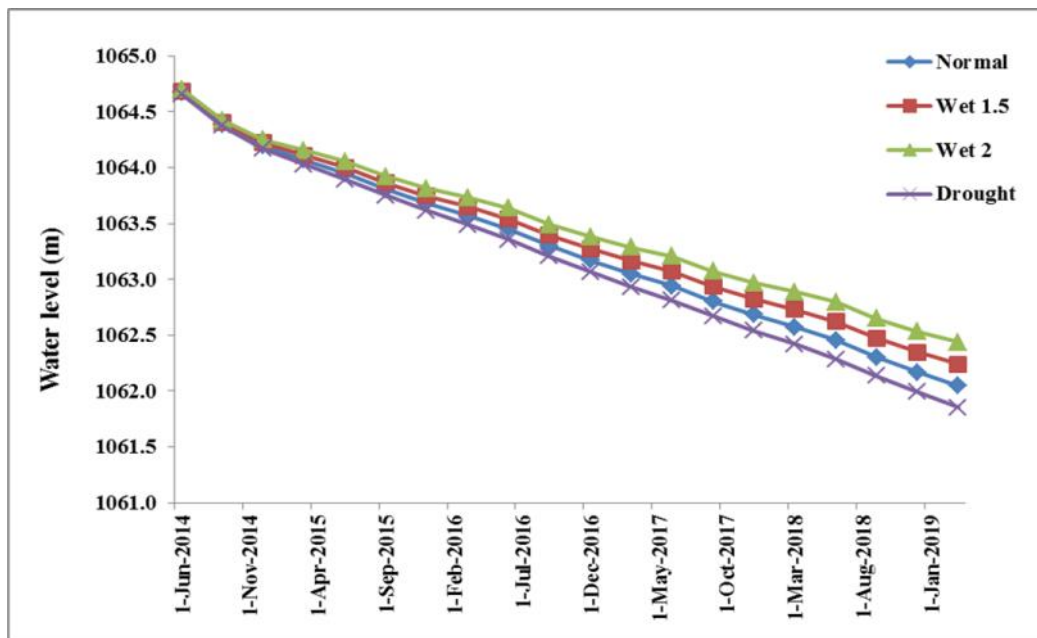


Figure 14. Photo of a long wide crack formed due to land subsidence in the Damghan plain

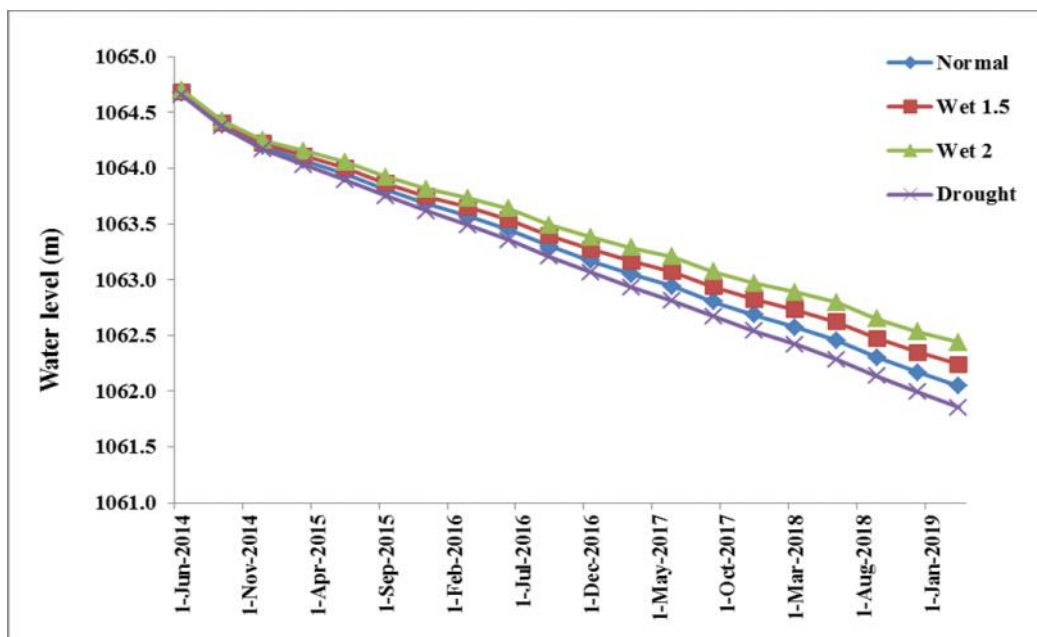


Figure 15. Average water level elevation in the subsidence area south of the Damghan plain

Land subsidence can occur under various conditions and on account of a variety of causes such as construction processes, vibration, and groundwater drawdown (Terzaghi, 1943; Hashemi, 2013). In the saturated soils, when the void water is decreased for some reason, the reducing space between the soil particles is not replaced by air (Kerh & Wu, 2003). Hence, there is reduction in the water pressure in the soil and as result of it we

have decreasing effective tension (Yoo *et al.*, 2008). In the study area, the main reason for land subsidence is the drastic groundwater drawdown in recent years, exacerbated by the type of lithology. As Figure 16 shows, there is 0.6 m/year drawdown in groundwater levels in this plain, and therefore, settlement is expected to increase in the future because of aquifer storage loss.

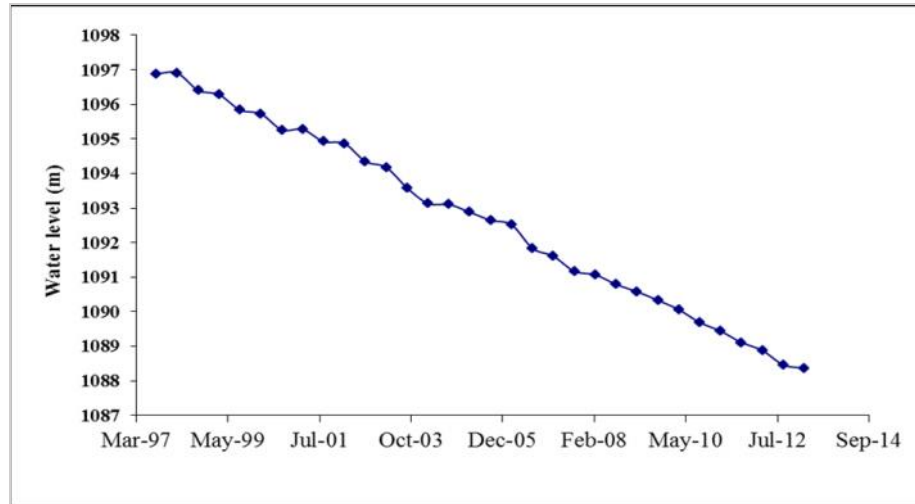


Figure 16. Average water level elevation in the Damghan aquifer during 1997–2013

Gene-Expression Programming model

Gene-Expression Programming (GEP) is a genotype/phenotype genetic algorithm that has been introduced by Ferreira (2001). It mainly inherits its characteristics from the genetic algorithm (GA) and genetic programming (GP). GEP can be used for the creation of computer programs (Mitchell, 1996; Ferreira, 2001). This technique is different from some of the other data-driven modeling techniques such as the artificial neural network (ANN) and the adaptive neuro-fuzzy inference system (ANFIS), in that, the derived model is not completely a “black-box” and the relationship between the input and the output can be expressed in a mathematical representation (Fernando *et al.*, 2012). This model

with its appreciable abilities can be a suitable tool for modeling nonlinear systems. The GEP model has been used by many researchers in hydrology, hydrogeology, and other engineering problems (Güven & Aytık, 2009; Zakaria *et al.*, 2010; Güven & Kisi, 2011; Kayadelen, 2011; Kisi & Shiri, 2012; Sattar, 2014). In this study, GEP has been used to predict land subsidence in the Damghan plain; together with Multiple Linear Regression (MLR), it has been employed to estimate the settlement from groundwater drawdown, by developing functional relations. Figure 17 shows the relation between groundwater drawdown and ground settlement in the period from 2010 to 2014.

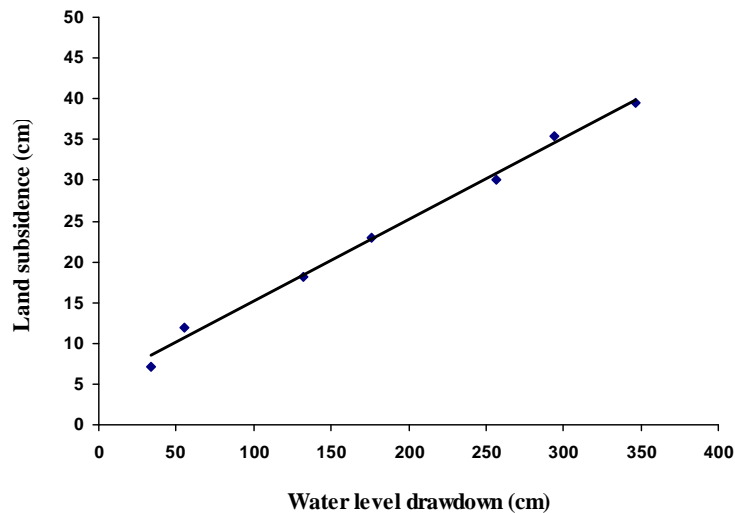


Figure 17. The correlation between water level drawdown and land subsidence (Source of filed data: Water Affairs Office of Damghan)

It should be noted that the field settlement data for this figure has been kindly provided by the Water Affairs Office of Damghan. Point-specific subsidence values are used to draw the figure, which corresponds to the location of the piezometers where the water level is measured.

The comparison between observed and estimated ground settlement is shown in Figure 18, in the form of a scatter plot. As displayed in this figure it was obvious that the predicted ground settlement follows very closely with the observed ground settlement for both models. However, when the performance of the GEP is compared with the MLR model in terms of performance measures (RMSE, MAE, R^2) it appears that the GEP performs better than MLR model with MAE = 1.235 cm, RMSE = 1.614 cm, and $R^2 = 0.990$, rather than MAE = 3.335 cm, RMSE = 3.452 cm, and $R^2 = 0.963$. In other words, the GEP reduced MAE and RMSE to 170 and 114%, respectively.

Therefore, the GEP model was used to develop the explicit equation and also to predict ground settlement in the next two years based on Equation 11, as follows:

$$S = \frac{4.46}{4.226 - 0.474h^{0.5}} + \frac{h - 10.972}{h^{0.25}} \quad (11)$$

where S is ground settlement in centimeters and h is groundwater drawdown in centimeters. The prediction shows that we have 35.4 cm and 39.45 cm settlement when the groundwater drawdown is 295 cm and 348 cm, respectively. The above figures show that the southern parts of the plain is more susceptible to subsidence and any increase in the groundwater overdraft will result in considerable subsidence. To accurately study and predict the settlement in this region, the model was repeatedly run for each piezometer in this area.

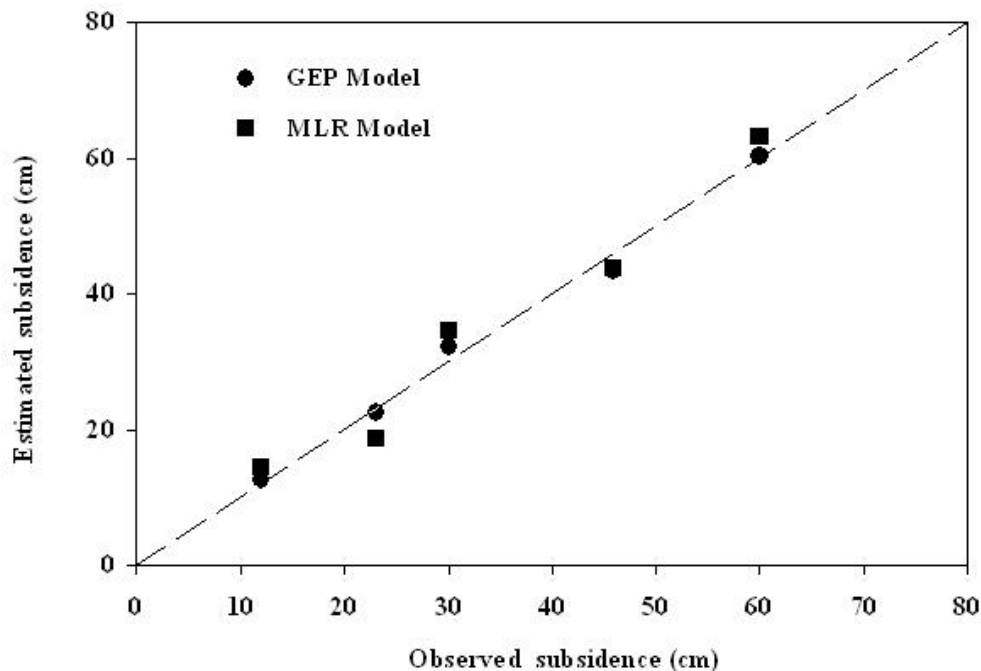


Figure 18. The correlation between estimated and predicted land subsidence on the basis of two developed models

Conclusions

The Damghan plain aquifer in northern Iran has been modeled by two different computer codes, GMS and GEP, to forecast water level drawdown and the associated land subsidence. The results show that,

a) Climate change exerts more influence in those

parts of the aquifer that are located close to the aquifer boundaries

b) There is a significant correlation between the rate of water level drawdown and the amount of land subsidence

c) The current groundwater abstraction rate will further intensify the drawdown and land subsidence

d) In the worst case scenario, where drought is exacerbated in the coming years, the maximum amount of water level drawdown and land subsidence in the next five years will be 3.43 m and 77 cm, respectively.

This research has clearly demonstrated that the current groundwater abstraction rates are not sustainable and should be substantially reduced even if rainfall increases to as much as two times that of the current annual average.

References

- Abbas Nejad, A., 1998. Assessment of environmental geology issues in Rafsanjani plain. In: Proceed of Second symposium of the Geological Society of Iran, Kerman pp 303–310.
- Alkhamis, R., Kariminasab, S., Aryana, F., 2006. Investigating the effect of land subsidence due to groundwater discharges on well casing damage. *Water and Wastewater* 60:77–88 (Persian with abstract in English).
- Bedekar, V., Niswonger, RG Kipp, K., Panday, S., Tonkin, M., 2012. Approaches to the simulation of unconfined flow and perched groundwater flow in MODFLOW. *Ground Water* 50:187–198.
- Bredehoeft J, Hall P (1995) Ground-water models. *Ground Water* 33:530–531.
- Cui, Y., Su, C., Shao, J., Wang, Y., Cao, X., 2014. Development and application of a regional land subsidence model for the Plain of Tianjin. *Journal of Earth Science*, 25(3):550–562.
- Deverel, SJ., Leighton, DA., 2010. Historic, recent and future subsidence, Sacramento-San Joaquin Delta, California, USA. *San Francisco Estuary and Watershed Science* 8(2):1–23.
- Elango, L., Senthil Kumar, M., 2006. Modeling the effect of sub-surface barrier on groundwater flow regime. In: Poeter EP, Zheng C, Hill MC (eds.), MODFLOW and More 2006: Managing groundwater systems. 806–810.
- Emamgholizadeh, S., Moslemi, K., Karami, G., 2014 Predicting of the groundwater level of Bastam Plain (Iran) by Artificial Neural Network (ANN) and Adaptive Neuro-Fuzzy Inference System (ANFIS). *Water Resour Manag* 28.
- Fatemi Aghda, M., Nakhaei, SM., Baitollahi, M., Aliyari, AR., 2001. Study of cause of sinkhole development in Hamedan central plain. In: Proceed of Second Iranian Conference of Engineering Geology and Environment, Tehran. 2: 693-701.
- Fernando, MJ., Burau, RG., Arulanandam, K., 1977. A new approach to determination of cation exchange capacity. *Soil Science American Journal*, 41:818–820.
- Ferreira, C., 2001. Gene expression programming: a new adaptive algorithm for solving problems. *Complex System* 13(2):87–129.
- Gerla, P.J., Matheney, R.K., 1996. Seasonal variability and simulation of groundwater flow in a prairie Wetland. *Hydrological Processes* 10:903–920.
- Ghafouri, MR., Shamohammadi, A., Kazemi, G.A., Moradi Harsini, K., Sharafi, H., 2013. Evaluation of the impact of groundwater levels drawdown on the instability and deterioration of water well screens. *Iran-Water Resources Research* 9:42–51 (Persian with abstract in English).
- Gurwin, J., Lubczynski, M., 2005. Modeling of complex multi-aquifer systems for groundwater resources evaluation—Swidnica study case (Poland). *Hydrogeol J*, 13:627–639.
- Güven, A., Aytekin, A., 2009. New approach for stage discharge relationship: gene expression programming. *Journal of Hydrologic Engineering*, 14: 812–820.
- Güven, A., Kisi, Ö., 2011. Estimation of suspended sediment yield in natural rivers using machine-coded linear genetic programming. *Water Resource Management*, 25:691–704.
- Huang, Y., Scanlon, B.R., Nicot, J.P., Reedy, R.C., Dutton, A.R., Kelley, V.A., Deeds, N.E., 2012. Sources of groundwater pumpage in a layered aquifer system in the Upper Gulf Coastal Plain, USA. *Hydrogeol J.*, 20:783–796.
- Kayadelen, C., 2011. Soil liquefaction modeling by Genetic Expression Programming and Neuro-Fuzzy. *Expert Systems with Applications*, 38(4): 4080–4087.
- Kisi, O., Shiri, J., 2012 River suspended sediment estimation by climatic variables implication: Comparative study among soft computing techniques. *Computers and Geosciences* 43:73–82.
- Kushwaha, RK., Pandit, M.K., Goyal, R., 2008. Groundwater management using groundwater modeling approach in northern part of Mendha Sub-basin, NE Rajasthan, India. In: *Groundwater Vision (Abstract Volume): International Groundwater Conference-2008 on Groundwater Dynamics & Global Change, India*. pp 127–128.
- Lashkaripour, G., R., Rostami Barani, H.R., Kohandel, A., Torshizi, H., 2006. Water level drawdown and land subsidence in Kashmar plain. In: Proceed. of 10th symposium of the Geological Society of Iran pp 2428–2438.
- Lewis, R.W., Schrefler, B., 2007. A fully coupled consolidation model of the subsidence of Venice. *Water Resource Res* 14(2):223–230.
- Li, W., Liu, Z., Guo, H., Li, N., Kang W., 2011. Simulation of a groundwater fall caused by geological discontinuities. *Hydrogeol J* 19:1121–1133.
- Louwyck, A., Vandenbohede, A., Bakker, M., Lebbe, L., 2014. MODFLOW procedure to simulate axisymmetric flow in radially heterogeneous and layered aquifer systems. *J Hydrol.* 22:1217–1226.

- Mitchell, M., 1996. An introduction to genetic algorithms, The MIT Press, Cambridge, p 221
- Mousavi, S.M., Shamsai, A., EI, Naggar, M.H., Khamehchian, M., 2001. A GPS-based monitoring program of land subsidence due to groundwater withdrawal in Iran. *Can. J. Civ. Eng.*, 28(3):452–464.
- Nastev, M., Rivera, A., Lefebvre, R., Martel, R., Savard, M., 2005. Numerical simulation of groundwater flow in regional rock aquifers, southwestern Quebec, Canada. *Hydrogeol J.*, 13:835–848.
- O’Sullivan, M., Yen, A., Clearwater, E., 2010. Three-dimensional model of subsidence at Wairakei-Tauhara. Auckland UniServices Limited, p 85.
- Ortega-Guerrero, A., Rudolph, DL., Cherry, J.A., 1999. Analysis of long-term land subsidence near Mexico City: Field investigation and predictive modeling. *Water Resour Res.*, 35(11): 3327–3341.
- Rahmanian, D., 1986. Land subsidence and development of earth cracks due to groundwater mining in Kerman. *Water* 36: 29-36.
- Rahnama, Rad, J., Firoozan, M., 2002. Investigating the impact of alternating droughts and erosion on buildings in large plain in Sistan. *Geotechnics and Strength of Materials Journal*. 88:30–39.
- Rejani, R., Jha, MK, Panda SN., Mull, R., 2008 Simulation modeling for efficient groundwater management in Balasore Coastal basin, India. *Water Resources Management Jour.*, 22: 23–50.
- Sakthivadivel, R., 2001. Artificial recharging of groundwater aquifers and groundwater modeling in the context of basin water management. In: Elango L, Jayakumar R (eds.) *Modeling in hydrology*, Allied Publishers Ltd, India. pp 36–37.
- Sattar, A., 2014. Gene Expression models for the prediction of longitudinal dispersion coefficients in transitional and turbulent pipe flow. *Journal of Pipeline Systems Engineering and Practice.*, 10.1061/(ASCE)PS.1949-1204.0000153, 04013011.
- Semnan Regional Water Company 2012. A report on groundwater resources in Damghan plain aquifer. Internal unpublished report.
- Sohrabi N, Chitsazan M, Amiri V, Maradi Neshd T (2013) Evaluation of groundwater resources in alluvial aquifer based on MODFLOW program, case study: Evan plain (Iran). *International Journal of Agriculture and Crop Sciences* 5(11):1164–1170.
- Sun, F., Shao, H., Kalbacher, T., Wang, W., Yang, Z., Huang, Z., Kolditz, O., 2011. Groundwater drawdown at Nankou site of Beijing Plain: model development and calibration. *Environ Earth Sci.*, 64:1323-1333.
- Tardast, A., Mousavi, M., Bolourchi, M.J., Shemshaki, A., 2011. Land subsidence due to water level decline in southwest Tehran. In: *Proceed. of fourth Water resources Management Conference*, Tehran.
- Regional Water Authority of Semnan, 2009. Hydrogeological report of Damghan plain.
- Varni MR, Usunoff EJ (1999) Simulation of regional-scale groundwater flow in the Azul River basin, Buenos Aires Province, Argentina. *Hydrogeol J* 7:180–187.
- Voss CI (2011) Editor’s message: Groundwater modeling fantasies–Part 1, adrift in the details. *Hydrogeol J* 19:1281–1284.
- Xue YQ, Zhang Y, Ye SJ, Wu JC, Li QF (2005) Land subsidence in China. *Environ Geol* 48(6): 713–720.
- Yidana SM (2011) Groundwater flow modeling and particle tracking for chemical transport in the southern Voltaian aquifers. *Environ Earth Sci* 63:709–721.
- Zakaria, N.A., Azamathulla, H.M.d., Chang, C.K., Ghani, A.A., 2010. Gene expression programming for total bed material load estimation—a case study. *Science of the Total Environment*, 408: 5078–5085.